Jurnal Ilmu Fisika
Vol. 15, No. 1, March 2023, hal. 48–55
ISSN: 1979-4657 (Print); 2614-7386 (Online)
https://doi.org/10.25077/jif.15.1.48-55.2023

Jurnal Ilmu Fisika
Open Access

Dosimetry Verification of Anisotropic Analytical Algorithm (AAA) in Eclipse Treatment Planning System (TPS) Based on Multileaf Collimator Variations

Fadillah Ahmad[1], Afdhal Muttaqin[1*], Dian Fitriyani[1], Ridwan Ridwan[2]
[1] Department of Physics, Faculty of Mathematics and Natural Sciences, Andalas University, Pauh, Padang 25163, Indonesia
[2] Siemens Healthineers Indonesia, Arkadia Office Park, Jakarta 12520, Indonesia

Article Info

Article History:

Received October 10, 2022
Revised December 19, 2022
Accepted December 30, 2022
Available online December 30, 2022

Keywords:

Anisotropic Analytical Algorithm
Dosimetry Verification
Treatment Planning System
Eclipse
Multileaf Collimator

Corresponding Author:

Afdhal Muttaqin
Email: allzputra@gmail.com

ABSTRACT

Dosimetry verification of anisotropic analytical (AAA) algorithms based on variations of the multileaf collimator has been investigated using the Eclipse Treatment Planning System. This study used a 0.6cc ionization chamber farmer detector and Linac Clinical CX variant equipped with TPS Eclipse with AAA. This study used 6 MV energy and 2 Gy dose. The multileaf collimator was varied into six groups with the size (A, B, C, D, E, F) of the irradiation field used 20 cm x 20 cm. The measurement results were a dose deviation value or a dose ratio presentation in each irradiation area. The dose deviation of the multileaf collimator variation was A 0.86% for each group. Group B had 6.8%, Group C had -0.43%, Group D had 0.73%, Group E had 1.11%, and Group F had 0.84%. The mean dose deviation value for all multileaf collimator forms was 1.67%, where this value is within the tolerance value recommended by ICRU, namely 3-5%. The p-value in the Analysis of variance (ANOVA) for the entire group was 0.00. This data shows that there is no effect of variation in the multileaf collimator on the dose given.

1. INTRODUCTION

Verified treatment planning system (TPS) dosimetry is one of the processes for optimizing therapy by using quality assurance (QA). Verification TPS dosimetry in radiotherapy can compare the results of in-house TPS calculations with clinically implemented commercial TPS software (Mu'minah et al., 2015). The accuracy of the TPS assay calculation is dependent on the algorithm used. That's because the more complicated the algorithm, the faster time and space will be. (Handika et al., 2020).

TPS has several algorithms used in calculating the dose. Some algorithms for calculations include Collapsed Cone Convolution (CCC), Printed Circuit Board (PCB), Aucross XB, Aucross BV, Anisotropic Analytical Algorithm (AAA), Monte Carlo (MC), Superposition, Convulsion (Lu et al., 2013). AAA is a fast algorithm for calculating dose compared to others because it uses a multi-source model to represent clinical beam properties and a patient scatter model represented by a measured density of poly-energy kernels. The AAA configuration uses only analytical functions, significantly reducing computation time (Hasenbalg et al., 2007). The AAA analytical function is based on the contribution functions (fluence, energy deposition density function, and scattering density) defined separately for each energy influence component. Functions representing the energy fluence and main kernel and scattering components are expressed analytically. The convolution integral over the beamlet dimensions has also been solved analytically so that these analytical functions help in dose optimization (Gagné and Zavgorodni, 2007).

The dose optimization algorithm is designed to meet the chosen limits and objectives. Consequently, treatment planning consists of control points by adjusting the multileaf collimator (MLC) openings for various sizes and shapes. Irregularly shaped MLC apertures with small sub-aperture components are challenging from a dosimetric point of view, as counting, delivery, and measurement will be affected, for example, due to a lack of charged particle balance (CPE) (Das et al., 2008). Small MLC apertures are cumbersome due to the increased sensitivity of MLC positioning error (LoSasso et al., 1998). It has been shown that some dose calculation algorithms underestimate a given dose of small static MLC aperture (Fog et al., 2011). Therefore, treatment planning with fields consisting of small MLC openings may lead to discrepancies between the calculated and delivered dose distributions.

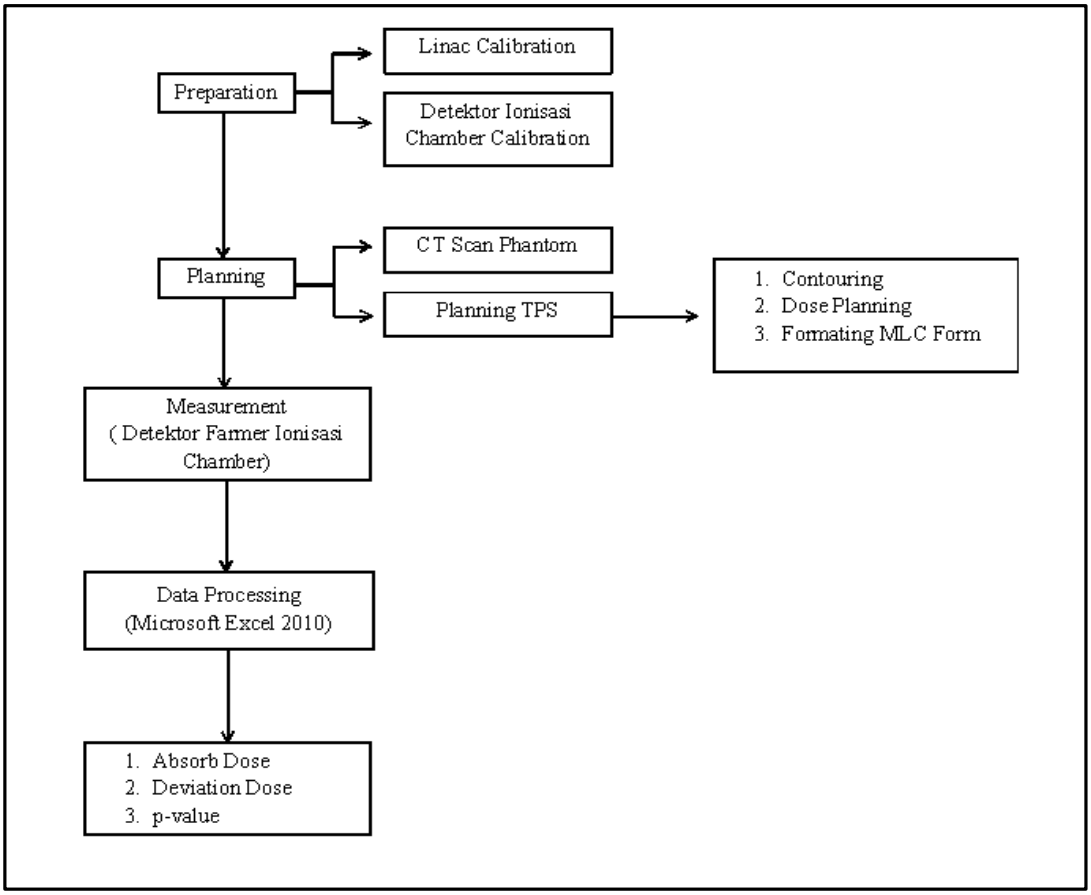

Figure 1. Research flowchart

Ridwan et al. (2017) researched the verification of dosimetry algorithms based on MLC aperture variations, resulting in MLC opening deviations of 0.95% A1, 1.23% A2, and -13.27% A3. MLC Aperture of groups B1 -0.30%, B2 -2.60% and B3 -1.72%. The MLC aperture of the C1 group was 0.63%, C2 0.72%, and C3 0.50%. MLC group D1 1.20%, D2 -1.55% and D3 -1.10%. Finally, in the MLC opening, group E produced E1 -1.07%, E2 -2.58%, and B3 -3.72%. The average dose deviation obtained was 1.47%. Verification of AAA dosimetry based on a variation of MLC shape has not been carried out. AAA was developed to improve dose calculation accuracy, especially in heterogeneous media (Van Esch et al., 2006). So this study aims to obtain information on verifying AAA dosimetry's accuracy in dosing with several forms of MLC.

2. METHOD

2.1 Research flow

This research was conducted in the radiotherapy room of Andalas University General Hospital. Based on Figure 1, the research preparation was initiated by calibrating the 0.6cc ionization

chamber farmer detector and the Linac Clinical CX variant equipped with TPS Eclipse with an anisotropic analytical (AAA) algorithm. Calibration is carried out to ensure that the results of measurements or checks carried out by the tool are accurate and consistent.

The phantom is then scanned using the CT-Simulator before being measured. Scanning of the phantom is carried out by inserting the detector into the hole in the phantom, then inserting the phantom into the CT-Simulator for scanning. The detector on the phantom is a reference point and target volume. The results of the slab phantom image obtained from the scan are sent to the TPS Eclipse software. Then the contouring process and radiation planning are carried out, namely the size of the irradiation area to be carried out, determining the table when placing the phantom when using LINAC, determining the energy, the dose to be used in TPS and the MLC form to be used. Scanning on a phantom is important for planning purposes where reference points and target volumes can be known. The measurement is a point dose measurement done right at the isocenter or point. Radiation dose measurements used a 0.6 cc farmer ionization chamber detector of 2.59 cm x 0.695 cm. The measurement results are processed using manual processing (Microsoft Excel 2010). The data processing results are obtained from dose deviation and p-value. The final stage is to compare the results of the initial planning with the resulting dose.

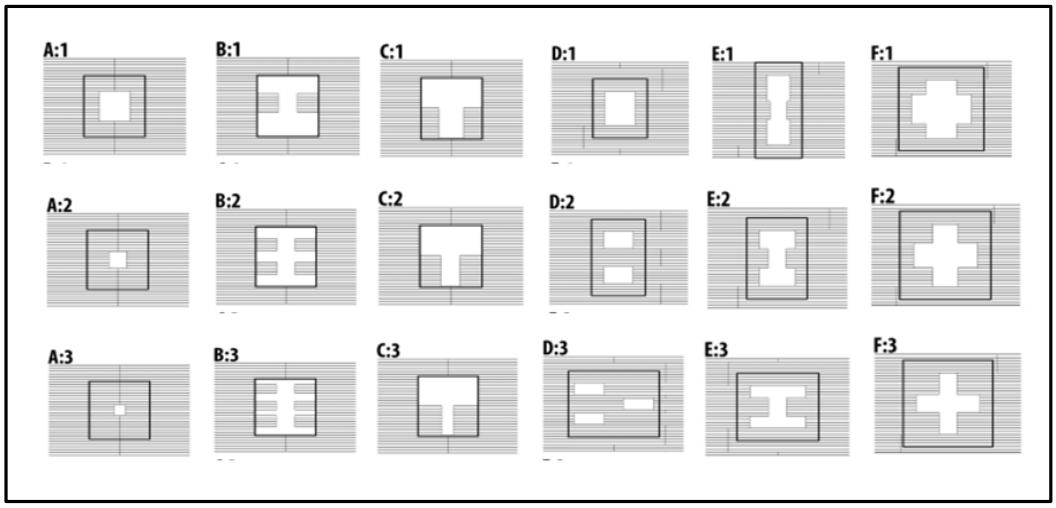

Figure 2. MLC Forms

2.2 Data

This research was carried out by varying the MLC aperture and using 6 MV of energy, a radiation dose of 2 Gy TPS, and an irradiation area of 20 cm x 20 cm, with target depth (d) 5 cm. The irradiation technique is a fixed SSD technique, with a source-to-surface distance (SSD) adjusted to the results of the planning at the TPS. The MLC forms used are divided into six groups, namely A, B, C, D, E, and F, where the forms This MLC is referenced based on research by Götstedt et al. (2015), which classifies MLC forms based on the addition or subtraction of MLC openings. The MLC form is shown in Figure 2.

2.3 Data Processing

The data processing in this study is by calculating the dose deviation by comparing the dose calculated by the TPS with the dose measured in the phantom as shown in Equation.1. The ρ-Value value is calculated using Equation.2.

$$\delta dosis(\%) = \frac{Dosis_{\text{calculated}} - Dosis_{TPS}}{Dosis_{TPS}} x100\% \quad (1)$$

TPS Dose is the TPS calculated dose, the measured dose is the estimated dose (Gy)

$$\rho - value = \frac{x_{sb}^2}{x_{sw}^2} \quad (2)$$

ρ-value is the probability, x^2sb is the mean of the squares between groups, and x^2sw is the mean of the squares between the groups.

3. RESULTS AND DISCUSSION

3.1 Absorb Dose

The irradiation results produced the absorbed dose value. Based on the results of measuring the average absorbed dose in groups A, D, E, and F according to the planned dose (Table 1). Measurements in group B experienced an increase of approximately 10% in absorbed dose results. Measurements in group B experienced an increase of approximately 10% in the results of the absorbed dose. Group B was dominated by an overestimated pattern (the measured dose was higher than the planned dose). If the planned dose of radiation received is not appropriate, then normal cells around cancer will receive radiation that is not needed so it will cause damage to these normal cells (Handayani et al. 2016).

Table 1. Average absorbed dose in each MLC

No	MLC Forms	Average (Gy)
1	A1	2.012
2	A2	2.013
3	A3	2.029
4	B1	2.132
5	B2	2.131
6	B3	2.145
7	C1	1.989
8	C2	1.991
9	C3	1.994
10	D1	2.015
11	D2	2.014
12	D3	2.015
13	E1	2.013
14	E2	2.026
15	E3	2.028
16	F1	2.014
17	F2	2.019
18	F3	2.018
Average		2.033

The increase in the absorbed dose produced in the MLC B form was due to the small opening area in group B resulting in a larger or inaccurate absorption dose. The small MLC area aperture is error-prone, especially if the aperture width field is only one to three (Brezovich et al. 2019). Research (Götstedt et al., 2015) that researched the development and evaluation of aperture-based complexity metrics using film and EPID measurements of static MLC apertures obtained inaccuracies for small area aperture sizes detected, the smallest MLC has a higher output level than the expected to result in a higher absorption dose.

Meanwhile, group C experienced a decrease of approximately 13%, and the measured dose dominated group C was lower than the planned dose. This is due to several things; first, the size of the MLC opening area is larger and causes the size of the ionization chamber to be smaller, 2.59 cm x 0.695 cm. The size of the ionization chamber must be proportional to the size of the radiation area so as not to experience a decrease in spatial resolution or the effect of volume averaging. Second, the charge particle equilibrium is not fulfilled due to the size of the radiation field opening, which is not

proportional to the electron distance on the lateral side, resulting in a lateral electronic disequilibrium (Underwood., 2013).

Increases and decreases in the absorbed dose can change cancer control and normal tissue. A 5% change in dose can result in a 10% to 20% change in the probability of both tumor control and cancer. Similarly, a 5% change in dose can result in a 20% to 30% change in the normal tissue complication rate (Ramdani and Haryanto, 2016). The difference in presentation is due to tissue differences between normal, cancerous, and tumor tissues.

Based on the data, the average absorbed dose of all MLC groups was 2.03 Gy, implying that the absorbed dose measurement results were compatible and that all MLC form parameters delivered the correct dose to the target. The planned dose is 2 Gy for each irradiation area. The average absorbed dose can be seen in Table 1. The resulting average absorbed dose is then evaluated to find the deviation value in the dose so that the measured dose deviation is obtained from the planned dose for each irradiation area.

3.2 Dose Deviation

The results of the evaluation of the absorbed dose resulted in deviations in the group (A, C, D, E, F) (Figure 3). The irradiation area with MLC group A1 resulted in a dose deviation of 0.60%, A2 of 0.65%, and A3 of 1.43%. The irradiation area with MLC group B1 resulted in a dose deviation of 6.58%, B2 6.57%, and B3 7.25%. The difference in dose deviation obtained in the irradiation area with the MLC form of group C1 was -0.55%, C2 was -0.45%, and C3 was -30%. The aperture of the MLC group D1 resulted in a dose deviation of 0.77%, D2 was 0.70%, and D3 was 0.75%. The MLC aperture in the E1 group yielded 0.63%, E2 1.30%, and E3 1.42%. Group F1 was 0.70%, F2 was 0.93% and F3 was 0.90%.

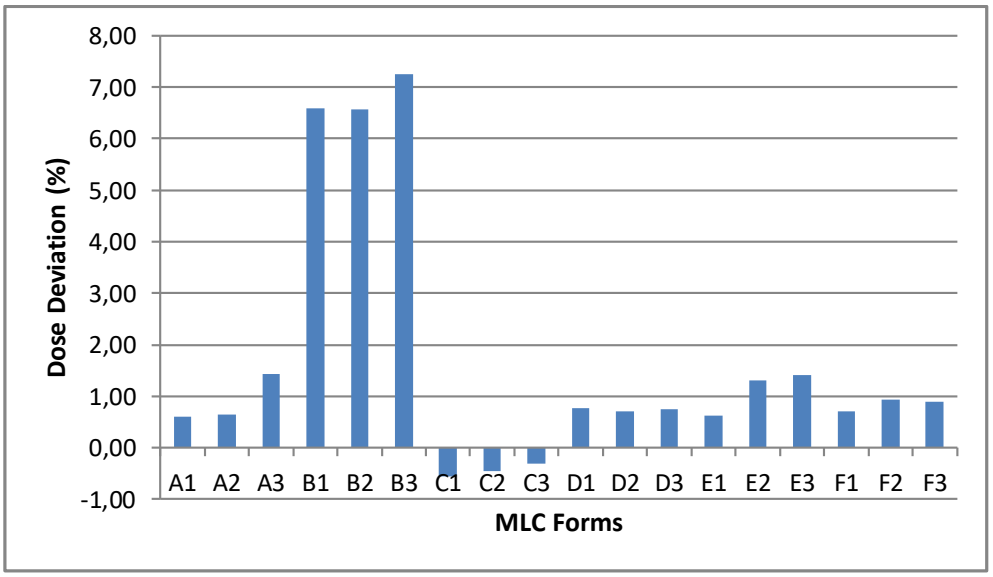

Figure 3. Average dose deviation for each form of MLC

The deviation results in the group (A, C, D, E, F) are below the tolerance range. Group B got a dose deviation above the tolerance range because the resulting absorbed dose also exceeded the planned absorbed dose. The deviation of the dose obtained can be seen in Table 1. Plus-minus in the results obtained has a meaning minus sign of the target dose under dose conditions. A positive sign indicates that the target dose has the appropriate dose or is overdosed (Suharsono., 2012).

Overall, the average dose deviation value for all forms of MLC in this study was 1.67%, indicating that the planned dose and the dose received remained within the recommended tolerance range, implying that the ability of LINAC with the TPS Eclipse type in administration accurately measured dose. The tolerance range recommended by the ICRU is 3-5% (ICRU., 1976). The results

differ from previous studies that measured using a farmer ionization chamber. Research by Rutonjski et al. (2012) measured the radiation dose in therapeutic planning using a farmer ionization chamber on a phantom. The calculated dose deviation was estimated to be less than 2% for 6 MV photons passing through a phantom equivalent to 5 cm thick water, while the bone equivalent material was up to 7% for energy 6 MVs and 15 MVs. The research of Götstedt et al. (2015) measured deviation by varying the shape of the MLC to get a deviation of 5%, which is still within the recommended tolerance range. The obtained dose deviation graph can be seen in Figure 3.

The difference in dose deviation obtained is based on the absorbed dose. The algorithm influences its use because the accuracy of dose calculation at TPS is influenced by the algorithm used. This study uses AAA. The AAA dose calculation model is a 3D pencil beam convolution-superposition algorithm with separate modeling for primary photons, secondary photons, and contamination electrons (Sievinen et al., 2005).

This study used AAA compared with similar studies but using different algorithms; both showed deviation values below the tolerance limit value. Suwandi et al. (2016) carried out dose measurements with AAA. They got the results that AAA generally gave better results in calculating point doses than convolution and superposition algorithms so AAA could be used as an accurate algorithm in clinical dose calculations.

The process of calculating clinical doses takes a fast time. AAA is a fast algorithm for calculating the dose because it uses analytical functions. AAA is a pencil beam convolution/superposition algorithm that uses a multi-source model to represent clinical beam properties and a patient scatters model represented by a measured density of poly-energy kernels. AAA uses only analytical functions that make analytical convolution possible and significantly reduce computational time (Hasenbalg et al., 2007). In addition, the difference between AAA and other algorithms is that AAA depends on the scattering core of the beam and is evaluated in various directions laterally from the beam. In addition, photon scattering is deflected with the core density scale along the beam direction to more accurately reproduce the dose at the heterogeneity boundary (Gagné and Zavgorodni, 2007). AAA can provide better results in dose calculations because the accuracy of the dose calculation algorithm on TPS depends on how detailed the modeling is on the physical particle transport process, which can simplify the procedure by describing particle transport to speed up calculations (Handika et al., 2020).

Table 2 . ρ-value calculation results

No	MLC Form	ρ-Value Between Groups	Overall -ρ Value
1	Group A	0.2220	0.0000
2	Group B	0.0008	
3	Group C	0.0025	
4	Group D	0.5120	
5	Group E	0.0000	
6	Group F	0.0003	

3.3 ρ-value

Based on the existing provisions, the p-value <0.05 indicates no effect of changing the dose and changes in the form of MLC. Groups (B, C, E, and F) produced p-value values smaller than 0.05, which means that there was no change in dose with the change of the MLC form. Groups (A and D) had a p-value value higher than the limit, meaning that the MLC form of groups (A and D) resulted in

a change in dose along with the difference in the MLC form. The ρ-value obtained can be seen in Table 1.

The cause of the difference in the results obtained is influenced by the difference in the size and shape of the irradiation area used. The A and D forms of MLC have a change in the MLC opening area or the irradiation area, which causes a difference in the results of the absorbed dose received. In Groups B, C, E, and F, changes in the size of the MLC openings are present but not too significant, which makes the results of the absorbed dose receive no change. Changes in dose and changes in the shape of the MLC, due to the presence of MLC, the irradiation area will decrease or increase so that the scattering of the phantom received by the dosimetry ionization chamber will also reduce or increase. (Jursinic., 1999).

Different results were obtained in the p-value of all forms of MLC. The results of the p-value calculation on the overall form of MLC produce a p-value value smaller than the limit, which means that changing the shape of the MLC on the radiation dose delivered has no effect. The ρ-value of the overall group obtained can be seen in Table 2.

4. CONCLUSION

Based on the results of the dosimetry verification study on the eclipse TPS based on the variation of the MLC form using the farmer ionization chamber detector, it can be concluded that the dose deviation in the area size and depth of the target is 1.67%. The data shows that the dose deviation within the recommended tolerance value is 3-5%. The dose calculation process using AAA is quite accurate, as indicated by the dose deviation data calculated by the AAA software. TPS has met the requirements of clinical tolerance in TPS. The p-value in the Analysis of variance (ANOVA) also shows no variation effect in the multileaf collimator on the dose given.

ACKNOWLEDGEMENT

Thank you to the research funders who came from and applied research in MIPA no contract 29/UN.16.03.D/PP/FMIPA/2022 and Andalas University Hospital, especially the radiotherapy section, who has helped research and allowed the use of the tools used in this study.

REFERENCE

Brezovich, I. A., Wu, X., Popple, R. A., Covington, E., Cardan, R., Shen, S., Fiveash, J., Bredel, M., and Guthrie, B. (2019). Stereotactic radiosurgery with MLC-defined arcs: Verification of dosimetry, spatial accuracy, and end-to-end tests. *Journal of Applied Clinical Medical Physics* 20, 84-98. https://doi.org/10.1002/acm2.12583

Das, I. J., Ding, G. X., and Ahnesjö, A. (2008). Small fields: nonequilibrium radiation dosimetry. *Medical physics* 35, 206-215. https://doi.org/10.1118/1.2815356

Fog, L. S., Rasmussen, J. F., Aznar, M., Kjær-Kristoffersen, F., Vogelius, I. R., Engelholm, S. A., and Bangsgaard, J. P. (2011). A closer look at RapidArc® radiosurgery plans using very small fields. *Physics in Medicine Biology* 56, 1853. https://iopscience.iop.org/article/10.1088/0031-9155/56/6/020

Gagné, I. M., and Zavgorodni, S. (2007). Evaluation of the analytical anisotropic algorithm in an extreme water–lung interface phantom using Monte Carlo dose calculations. *Journal of Applied Clinical Medical Physics* 8, 33-46. https://doi.org/10.1120/jacmp.v8i1.2324

Götstedt, J., Karlsson Hauer, A., Bäck, and Anna (2015). Development and evaluation of aperture-based complexity metrics using film and EPID measurements of static MLC openings. *Medical physics* 42, 3911-3921. https://doi.org/10.1118/1.4921733

Handayani, M., Milvita, D., Herlinda, S., and Unand, J. J. F. (2016). Verifikasi Ketepatan Hasil Perencanaan Nilai Dosis Radiasi Terhadap Penerimaan Dosis Radiasi Pada Pasien Kanker. *Jurnal Fisika Unand* 5, 159-165. https://doi.org/10.25077/jfu.5.2.159-165.2016

Handika, A. D., Tarigan, S. T., Karunia, P. D., Syafi'i, A., Fauzia, A. R., Mar'ie, K., Pontoh, P. A., and Pawiro, S. A. (2020). Audit dosimetri treatment planning system berkas foton pada radioterapi eksternal: A Review. *Journal of Medical Physics Biophysics* 7, 32-45.

Hasenbalg, F., Neuenschwander, H., Mini, R., and Born, E. (2007). Collapsed cone and analytical anisotropic algorithm dose calculations compared to VMC++ Monte Carlo simulations in clinical cases. *Journal of Physics: Conference Series*, Vol. 74, pp. 021007. IOP Publishing. doi:10.1088/1742-6596/74/1/012007

ICRU (1976). *Determination of absorbed dose in a patient irradiated by beams of X- or gamma-rays in radiotherapy procedures*, Washington DC:.

Jursinic, P. A. (1999). Changes in incident photon fluence of 6 and 18 MV x rays caused by blocks and block trays. *Medical Physics* 26, 2092-2098. https://doi.org/10.1118/1.598724

LoSasso, T., Chui, C. S., and Ling, C. C. (1998). Physical and dosimetric aspects of a multileaf collimation system used in the dynamic mode for implementing intensity modulated radiotherapy. *Medical physics* 25, 1919-1927. https://doi.org/10.1118/1.598381

Lu, L., Yembi-Goma, G., Wang, J. Z., Gupta, N., Huang, Z., Lo, S. S., Martin, D., and Mayr, N. (2013). A practical method to evaluate and verify dose calculation algorithms in the treatment planning system of radiation therapy. *International Journal of Medical Physics, Clinical Engineering Radiation Oncology* 2, 76. http://dx.doi.org/10.4236/ijmpcero.2013.23011

Mu'minah, I. A., La Ode Husein, Z., Pawiro, and A, S. (2015). Verifikasi Dosimetri Perhitungan Berkas Terbuka Perangkat Lunak In-House Treatment Planning System (Tps) Pesawat Teleterapi Cobalt-60. *Prosiding Seminar Nasional Fisika (E-Journal)*, Vol. 4, pp. SNF2015-V-33-38. http://journal.unj.ac.id/unj/index.php/prosidingsnf/article/view/5144

Ramdani, R., and Haryanto, F. (2016). Perbandingan Dosis Serap Berkas Foton 16 MV Pada berbagai Jenis Phantom Menggunakan Metode Monte Carlo-EGSnrc. *Jurnal Wahana Fisika*, 129-139.

Ridwan, Supriyanto Arjo Pawiro, and Soejoko, D. (2017). Development and evaluation of complexity metric of static MLC openings of linear accelerator. *Congress of medical physics*.

Rutonjski, L., Petrović, B., Baucal, M., Teodorović, M., Čudić, O., Gershkevitsh, E., and Izewska, J. (2012). Dosimetric verification of radiotherapy treatment planning systems in Serbia: national audit. *Radiation Oncology* **7**, 1-8.

Sievinen, J., Ulmer, W., and Kaissl, W. (2005). AAA photon dose calculation model in eclipse. *Palo Alto : Varian Medical Systems* **118**, 2894.

Suharmono, B. H., Anggraini, I. Y., Hilmaniyya, H., and Astuti, S. D. (2020). Quality Assurance (QA) Dan Quality Control (QC) Pada Instrumen Radioterapi Pesawat LINAC. *J Jurnal Biosains Pascasarjana* 22, 73-80. https://doi.org/10.20473/jbp.v22i2.2020.73-80

Suharsono (2012). *Verifikasi dosis radioterapi eksterna metode in vivo pada phantom*, Universitas Indonesia, Depok.

Suwandi, Wibowo, W. E., Pawiro, and Ardjo, S. (2016). Simulasi Audit Dosimetri Treatment Planning System Foton Sinar-X 6 Mv Multicenter Radioterapi. *Prosiding Seminar Nasional Fisika (E-Journal)*, Vol. 5, pp. SNF2016-BMP-23-28. https://doi.org/10.21009/0305020305

Underwood, R. J. (2013). Small field dose calibrations with gafchromic film. no. May, 73.

Van Esch, A., Tillikainen, L., Pyykkonen, J., Tenhunen, M., Helminen, H., Siljamäki, S., Alakuijala, J., Paiusco, M., Iori, M., and Huyskens, D. P. (2006). Testing of the analytical anisotropic algorithm for photon dose calculation. *Medical physics* 33, 4130-4148. https://doi.org/10.1118/1.2358333